Available online at www.sciencedirect.com
SCIENCE DIRECT®
Journal of Power Sources 119–121 (2003) 959–963
JOURNAL OF POWER SOURCES
www.elsevier.com/locate/jpowsour

Three-volt lithium-ion battery with $Li[Ni_{1/2}Mn_{3/2}]O_4$ and the zero-strain insertion material of $Li[Li_{1/3}Ti_{5/3}]O_4$

Kingo Ariyoshi, Satoshi Yamamoto, Tsutomu Ohzuku*

Electrochemistry and Inorganic Chemistry Laboratory, Department of Applied Chemistry, Graduate School of Engineering, Osaka City University (OCU), Sugimoto 3-3-138, Sumiyoshi, Osaka 558-8585, Japan

Abstract

A 3 V lithium-ion cell with $Li[Ni_{1/2}Mn_{3/2}]O_4$ ($Fd\bar{3}m$; $a = 8.17$ Å) and the zero-strain insertion material of $Li[Li_{1/3}Ti_{5/3}]O_4$ ($Fd\bar{3}m$; $a = 8.36$ Å) was examined with an emphasis on rate-capability and cycle life. This cell showed a quite flat operating voltage of 3.2 V with excellent cycleability. Accelerated cycle tests indicated that 83% of the initial capacity was delivered and stored even after 1100 cycles. Although the calculated energy density of a $Li[Li_{1/3}Ti_{5/3}]O_4/Li[Ni_{1/2}Mn_{3/2}]O_4$ cell was about 250 Wh kg^{-1} or 1000 Wh dm^{-3} based on the active material weight or volume, the 3 V lithium-ion battery exhibited positive characteristic features, such as flatness in operating voltage, high rate capability, and cycle life.

Keywords: Lithium-ion cell; Lithium nickel manganese oxide; Lithium titanium oxide

1. Introduction

Lithium-ion batteries normally consist of $LiCoO_2$ and graphite, so that operating voltages are somewhere between 3.0 and 4.2 V. However, one of the advantages of lithium-ion technology is that one can design the operating voltage including its profile by the selection of lithium insertion materials. In this paper, we report a 3 V lithium-ion battery showing an extremely flat operating voltage of 3.2 V, which is equivalent to two Zn/Ag_2O cells connected in series, with excellent rechargeability.

The negative-electrode material we selected was a so-called zero-strain insertion material of $Li[Li_{1/3}Ti_{5/3}]O_4$ [1], because it showed a flat, reliable operating voltage of 1.55 V against a lithium electrode and virtually no limitation on cycle life [1,2]. A positive electrode improved for this purpose was a so-called 5 V lithium insertion material [3], specifically $Li[Ni_{1/2}Mn_{3/2}]O_4$ having a spinel-framework structure [3,4].

The objective of this research is to show whether or not such a 3 V lithium-ion battery with $Li[Ni_{1/2}Mn_{3/2}]O_4$ and $Li[Li_{1/3}Ti_{5/3}]O_4$ is possible as an alternative to 3 V application for which two alkaline secondary batteries connecting in series are currently applied.

2. Experimental

The starting material used to prepare $Li[Ni_{1/2}Mn_{3/2}]O_4$ was a nickel manganese double hydroxide (MX-003-2; Ni:Mn = 1.01:2.99 in molar ratio) obtained from Tanaka Chemical Corp., Ltd., Japan [5]. The reaction mixture with lithium hydroxide was pressed into pellets (23 mm diameter and ca. 5 mm thick.) and heated at 1000 °C for 12 h followed by heating at 700 °C for 48 h in air [6]. The reaction product was ground using mortar with a pestle and stored in a desiccator over blue silica-gel before use. X-ray diffraction (XRD) data were obtained by using an X-ray diffractometer (Type XD-3A, Shimadzu Corp., Ltd.) with Cu Kα radiation, equipped with a diffracted beam graphite monochromator. Fourier-transform infrared (FT-IR) spectra of the samples were obtained by a KBr method using a FT-IR spectrometer 8300 (Shimadzu Corp., Ltd.).

Electrochemical cells used were the same as described previously [7]. Polyvinylidene fluoride (PVdF) was used as a binder to prepare electrodes. Black viscous slurry consisting of 80 wt.% $Li[Ni_{1/2}Mn_{3/2}]O_4$ or $Li[Li_{1/3}Ti_{5/3}]O_4$, 10 wt.% acetylene black (AB), and 10 wt.% PVdF dispersed in *N*-methyl-2-pyrrolidone (NMP) was cast on aluminum foil with a blade, and NMP was evaporated at room temperature in air, then under vacuum at 60 °C for 30 min, and finally the electrodes (15 mm × 20 mm) were dried under vacuum at 150 °C for 14 h. A lithium electrode

* Corresponding author.
E-mail address: ohzuku@a-chem.eng.osaka-cu.ac.jp (T. Ohzuku).

0378-7753/03/$ – see front matter
doi:10.1016/S0378-7753(03)00298-2

was prepared by pressing a lithium metal sheet onto a stainless steel plate (15 mm × 20 mm). Two sheets of polypropylene micro-porous membrane (Celgard 2500) were used as a separator. Electrolyte used was 1 M $LiPF_6$ dissolved in ethylene carbonate (EC)/dimethyl carbonate (DMC) (3/7 by volume) solution. In fabricating the cells, all materials except the electrolyte and lithium metal were dried under vacuum at 60 °C for at least 2 h to avoid possible contamination of water. For the electrochemical tests the current applied to the cell was 0.5 mA, which corresponded to the current density of 0.17 mA cm^{-2} unless otherwise noted. Other sets of experimental conditions are given in Section 3.

3. Results and discussion

Fig. 1 shows the XRD patterns of (a) $Li[Ni_{1/2}Mn_{3/2}]O_4$ and (b) $Li[Li_{1/3}Ti_{5/3}]O_4$. All diffraction lines of both samples could be indexed by assuming a cubic lattice. Lattice parameters, $a = 8.17$ Å for (a) and $a = 8.36$ Å for (b), were obtained by a least squares method using 14 diffraction lines. Both structures were primarily identified as a spinel-framework structure having a space group of $Fd\bar{3}m$. In the spinel-framework structure the oxygen ions at the 32(e) sites form

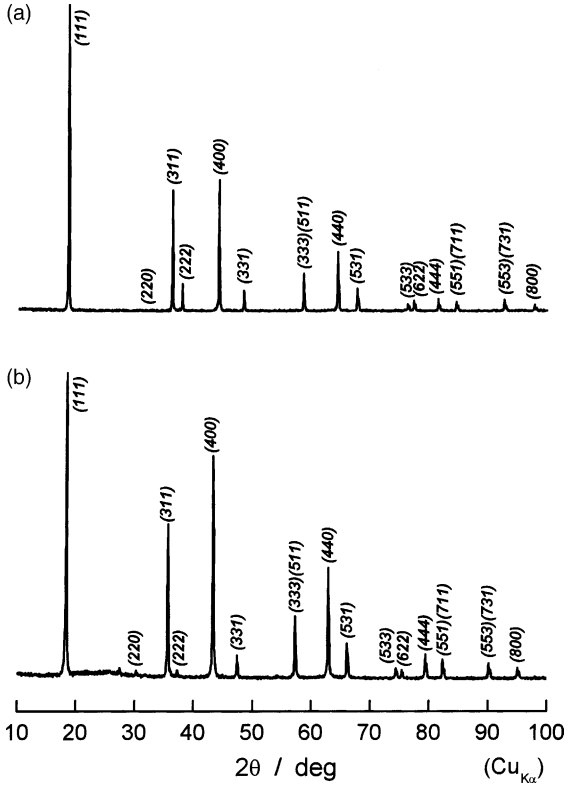

Fig. 1. XRD patterns of (a) $Li[Ni_{1/2}Mn_{3/2}]O_4$ ($a = 8.17$ Å), and (b) $Li[Li_{1/3}Ti_{5/3}]O_4$ ($a = 8.36$ Å). $Li[Ni_{1/2}Mn_{3/2}]O_4$ was prepared by heating a reaction mixture at 1000 °C for 12 h followed by heating at 700 °C for 48 h in air.

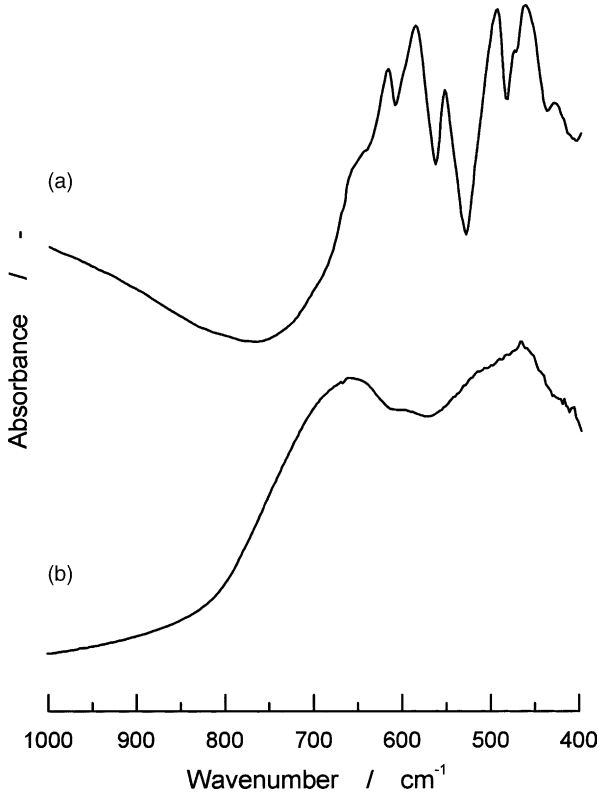

Fig. 2. IR spectra of (a) $Li[Ni_{1/2}Mn_{3/2}]O_4$, and (b) $Li[Li_{1/3}Ti_{5/3}]O_4$. The samples are the same as described in Fig. 1(a) and (b).

the cubic-close packing, in which the cations normally occupy the tetrahedral and octahedral interstices. In $Li[Ni_{1/2}Mn_{3/2}]O_4$ nickel and manganese ions supposedly distribute the 16(d) sites by the ratio of Ni/Mn = 1/3. For $Li[Li_{1/3}Ti_{5/3}]O_4$ lithium and titanium ions randomly occupy at the 16(d) sites by the ratio of Li/Ti = 1/5. For both samples the tetrahedral 8(a) sites are usually occupied by lithium ions. The difference between two is a distribution of cations at the 16(d) sites. To illustrate the specific crystal structures of both $Li[Ni_{1/2}Mn_{3/2}]O_4$ and $Li[Li_{1/3}Ti_{5/3}]O_4$ is out of the scope of this paper.

The FT-IR spectra of (a) $Li[Ni_{1/2}Mn_{3/2}]O_4$ and (b) $Li[Li_{1/3}Ti_{5/3}]O_4$ are shown in Fig. 2. A fine-structure consisting of at least eight absorption bands in the range of 400–800 cm^{-1} is characteristic of battery-active $Li[Ni_{1/2}Mn_{3/2}]O_4$ [6]. Although the XRD pattern of $Li[Li_{1/3}Ti_{5/3}]O_4$ is quite similar to that of $Li[Ni_{1/2}Mn_{3/2}]O_4$, $Li[Li_{1/3}Ti_{5/3}]O_4$ shows ill-defined absorption bands at 660 and 470 cm^{-1}.

Fig. 3 shows the charge and discharge curves of (a) Li/$Li[Ni_{1/2}Mn_{3/2}]O_4$, (b) Li/$Li[Li_{1/3}Ti_{5/3}]O_4$, and (c) a lithium-ion cell of the combinations of $Li[Ni_{1/2}Mn_{3/2}]O_4$ and $Li[Li_{1/3}Ti_{5/3}]O_4$. In Fig. 3 almost steady voltage curves were illustrated. As clearly seen in Fig. 3(a) and (b), the operating voltages of lithium cells with $Li[Ni_{1/2}Mn_{3/2}]O_4$ or $Li[Li_{1/3}Ti_{5/3}]O_4$ are extremely flat, i.e. 4.72 V for $Li[Ni_{1/2}Mn_{3/2}]O_4$ and 1.55 V for $Li[Li_{1/3}Ti_{5/3}]O_4$. Coulombic efficiency during charge and discharge of Li/$Li[Ni_{1/2}Mn_{3/2}]O_4$ (ca. 99%)

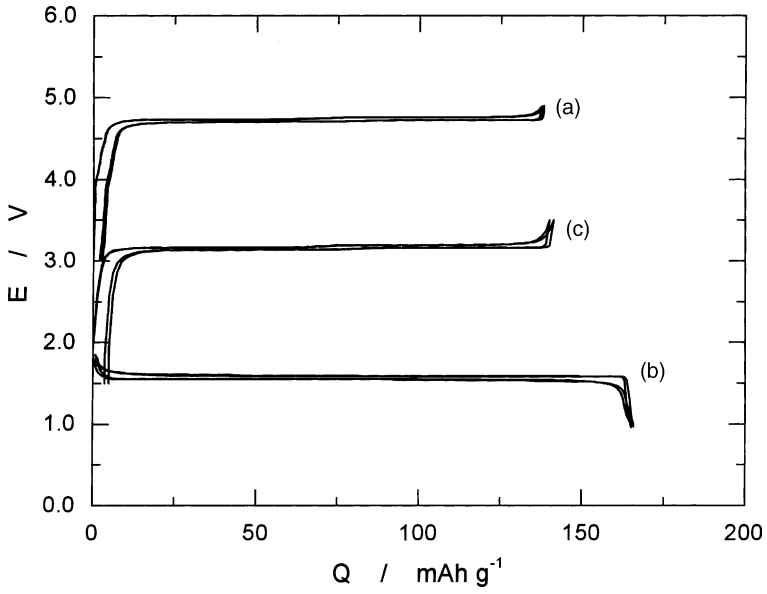

Fig. 3. Charge and discharge curves of (a) Li/Li[$Ni_{1/2}Mn_{3/2}$]O_4, (b) Li/Li[$Li_{1/3}Ti_{5/3}$]O_4, and (c) a lithium-ion cell with Li[$Ni_{1/2}Mn_{3/2}$]O_4 and Li[$Li_{1/3}Ti_{5/3}$]O_4. Cells were operated at a rate of 0.17 mA cm^{-2} at 30 °C.

was lower than that of Li/Li[$Li_{1/3}Ti_{5/3}$]O_4 (ca. 100%), suggesting instability of the electrolyte at high voltage region. As seen in Fig. 3(c), a 3 V lithium-ion cell is really possible by combining two lithium insertion materials based on lithiated transition metal oxides. The operating voltage of the Li[$Ni_{1/2}Mn_{3/2}$]O_4/Li[$Li_{1/3}Ti_{5/3}$]O_4 cell is 3.2 V which is two times higher than that of nickel/cadmium or nickel/metal hydride alkaline batteries or equivalent to that of Li/MnO_2 primary battery.

When we assume the following reaction to calculate theoretical capacities of this cell,

$$\mathrm{Li[Ni_{1/2}Mn_{3/2}]O_4 + Li[Li_{1/3}Ti_{5/3}]O_4 \rightarrow \square[Ni_{1/2}Mn_{3/2}]O_4 + Li_2[Li_{1/3}Ti_{5/3}]O_4},$$

the specific capacity is estimated to be 80 Ah kg^{-1} or 315 Ah dm^{-3} by using the values of $a = 8.17$ Å for Li[$Ni_{1/2}Mn_{3/2}$]O_4 and $a = 8.36$ Å for Li[$Li_{1/3}Ti_{5/3}$]O_4.

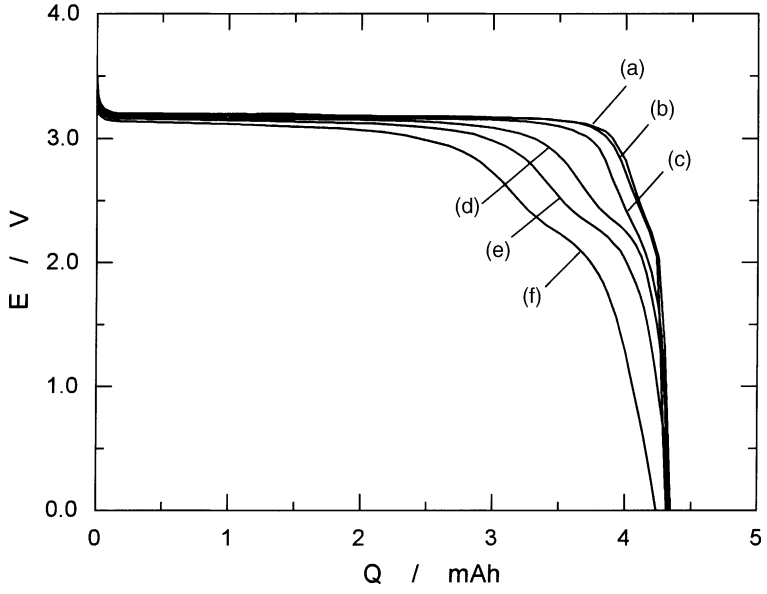

Fig. 4. Rate-capability tests on a lithium-ion cell with Li[$Li_{1/3}Ti_{5/3}$]O_4 (0.086 g) and Li[$Ni_{1/2}Mn_{3/2}$]O_4 (0.043 g). The cell was charged at 3.5 V until the current reduced to below 0.033 mA cm^{-2} and then discharged at (a) 0.10 mA cm^{-2} (8.8 mA g^{-1} based on Li[$Ni_{1/2}Mn_{3/2}$]O_4 sample weight), (b) 0.17 mA cm^{-2} (14.7 mA g^{-1}), (c) 0.33 mA cm^{-2} (29.4 mA g^{-1}), (d) 0.67 mA cm^{-2} (58.8 mA g^{-1}), (e) 1.0 mA cm^{-2} (88.2 mA g^{-1}), or (f) 1.67 mA cm^{-2} (147.1 mA g^{-1}).

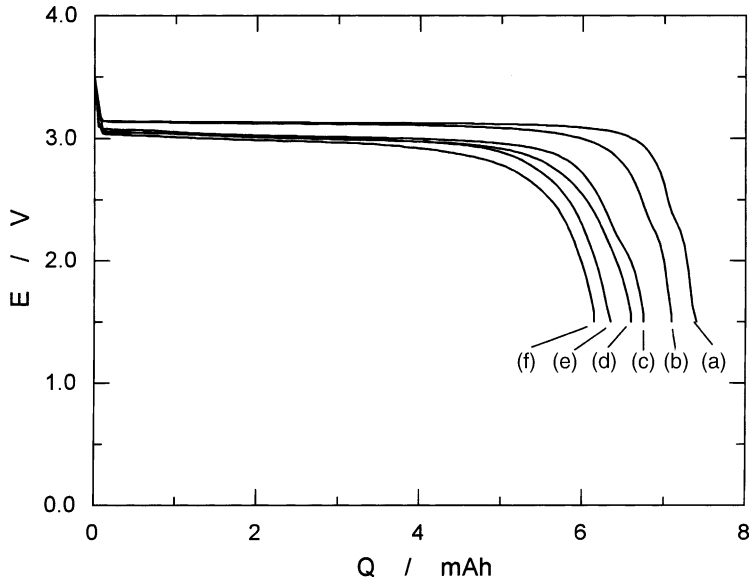

Fig. 5. Results on the accelerated cycle tests of a lithium-ion cell with $Li[Li_{1/3}Ti_{5/3}]O_4$ (0.074 g) and $Li[Ni_{1/2}Mn_{3/2}]O_4$ (0.070 g): (a) 3rd cycle, (b) 50th cycle, (c) 200th cycle, (d) 400th cycle, (e) 700th cycle, and (f) 1100th cycle. The cell was cycled under constant voltage charge at 3.5 V for 12 min and discharge at 1.5 V for 12 min. Voltage curves shown are from a constant-current reference cycle with a discharge rate of 0.6 mA cm^{-2} at 30 °C.

Consequently, the energy density of lithium-ion cell with $Li[Ni_{1/2}Mn_{3/2}]O_4$ and $Li[Li_{1/3}Ti_{5/3}]O_4$ is calculated to be 250 Wh kg^{-1} or 1000 Wh dm^{-3}.

Fig. 4 shows preliminary test results on the rate-capability for a cell with $Li[Li_{1/3}Ti_{5/3}]O_4$ and $Li[Ni_{1/2}Mn_{3/2}]O_4$. The discharge current was varied from 0.10 to 1.67 mA cm^{-2} corresponding to 8.8–147 mA g^{-1} based on $Li[Ni_{1/2}Mn_{3/2}]O_4$ sample weight. The cut-off voltage was selected to be 0 V for discharge. After each discharge, the cell was charged at constant voltage of 3.5 V until the current reduced below 0.033 mA cm^{-2}. As seen in Fig. 4, the discharge curves become reduced and an apparent inflection is observed at ca. 2.4 V for high-rates of discharge, which is not clear for the low rate discharge of (a), (b) or (c).

Results on the accelerated cycle tests are shown in Fig. 5. To accelerate cell cycles, a cell was cycled under constant voltage charge at 3.5 V for 12 min and discharge at 1.5 V for 12 min. Maximum charging current at 3.5 V was observed to

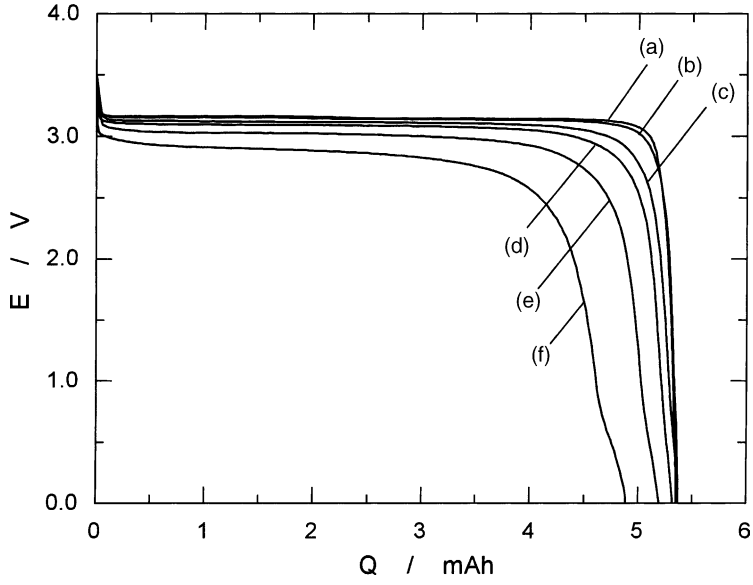

Fig. 6. Rate-capability tests on a lithium-ion cell with $Li[Li_{1/3}Ti_{5/3}]O_4$ (0.056 g) and $Li[Ni_{1/2}Mn_{3/2}]O_4$ (0.049 g). To improve rate-capability, $Li[Ni_{1/2}Mn_{3/2}]O_4$ was prepared by a fast cooling method. The cell was charged at constant voltage of 3.5 V until the current reduced to below 0.033 mA cm^{-2} and then discharged at (a) 0.17 mA cm^{-2} (12.7 mA g^{-1} based on $Li[Ni_{1/2}Mn_{3/2}]O_4$ sample weight), (b) 0.33 mA cm^{-2} (25.5 mA g^{-1}), (c) 1.0 mA cm^{-2} (76.4 mA g^{-1}), (d) 1.67 mA cm^{-2} (127 mA g^{-1}), (e) 3.33 mA cm^{-2} (255 mA g^{-1}), or (f) 6.67 mA cm^{-2} (509 mA g^{-1}).

be 60 mA cm^{-2} or 5 A g^{-1} based on the $Li[Ni_{1/2}Mn_{3/2}]O_4$ sample weight and the maximum discharging current was 100 mA cm^{-2} or 9 A g^{-1} based on $Li[Ni_{1/2}Mn_{3/2}]O_4$ in this case. The cell stored and delivered 20–70% of theoretical capacity depending on cycle number, i.e. 70% for 10th cycle, 60% for 50th, 35% for 200th, 30% for 400th, and 20% for 1100th cycle. To measure cell capacity as a function of cycle number selected, the cell was discharged at a rate of 0.6 mA cm^{-2} at 30 °C after the constant voltage charge at 3.5 V for approximately 5 h. As clearly seen in Fig. 5, 83% of initial capacity can be stored and delivered even after 1100 cycles. This indicates that the cycleability and rate-capability are expected to be excellent if we can improve the electrolyte and the processing method to prepare high-rate and long-life $Li[Ni_{1/2}Mn_{3/2}]O_4$.

To improve the rate-capability of $Li[Ni_{1/2}Mn_{3/2}]O_4$ more than that shown in Fig. 4, fast-cooling methods were examined. The processing method is the same as described in Section 2 except for the cooling and oxidation processes. After reacting the mixture at 1000 °C for 12 h, the sample was cooled down to room temperature by using a stainless steel plate. The obtained sample was crushed to powder, pressed into pellets again, and oxidized at 700 °C for 12 h. Fig. 6 shows the rate-capability tests of the cell with $Li[Li_{1/3}Ti_{5/3}]O_4$ and the obtained $Li[Ni_{1/2}Mn_{3/2}]O_4$ sample. Operating voltages are extremely flat even in high current operation, indicating that a lithium-ion cell with $Li[Li_{1/3}Ti_{5/3}]O_4$ and $Li[Ni_{1/2}Mn_{3/2}]O_4$ potentially has a power density as high as 0.67 kW kg^{-1} or 2.6 kW dm^{-3} with accessible energy densities of 250 Wh kg^{-1} or 1 kWh dm^{-3} based on the active materials weight or volume. $Li[Ni_{1/2}Mn_{3/2}]O_4$ prepared by a fast cooling method showed identical XRD and FT-IR signals to those shown in Figs. 1 and 2. The specific differences between these two samples are not known at present. High-resolution transmission electron microscopic observation with selected area electron diffraction will give more insights into their structures. Such an approach is under way in our laboratory.

Acknowledgements

One of us (T.O.) wishes to thank Mr. Hiroyuki Ito of Tanaka Chemical Corp., Ltd., Japan for his help on the preparation of nickel manganese double hydroxide. The present work was partially supported by a grant-in-aid from the Osaka City University (OCU) Science Foundation.

References

[1] T. Ohzuku, A. Ueda, N. Yamamoto, J. Electrochem. Soc. 142 (1995) 1431.
[2] K. Zaghib, M. Simoneau, M. Armand, M. Gauthier, J. Power Sources 81–82 (1999) 90.
[3] T. Ohzuku, S. Takeda, M. Iwanaga, J. Power Sources 81–82 (1999) 90, and references therein.
[4] Q. Zhong, A. Banakdorpour, M. Zhang, Y. Gao, J.R. Dahn, J. Electrochem. Soc. 144 (1997) 205.
[5] T. Ohzuku, K. Ariyoshi, S. Yamamoto, Y. Makimura, Chem. Lett. 1270 (2001).
[6] T. Ohzuku, K. Ariyoshi, S. Yamamoto, J. Ceram. Soc. Jpn. 110 (2002) 501.
[7] T. Ohzuku, A. Ueda, M. Nagayama, J. Electrochem. Soc. 140 (1994) 1241.